Published in final edited form as:
Biol Psychiatry. 2013 October 1; 74(7): 547–555. doi:10.1016/j.biopsych.2013.02.026.

A Selective Insular Perfusion Deficit Contributes to Compromised Salience Network Connectivity in Recovering Alcoholic Men

Edith V. Sullivan[1], **Eva Müller-Oehring**[1,2], **Anne-Lise Pitel**[1], **Sandra Chanraud**[1,2], **Ajit Shankaranarayanan**[3], **David C. Alsop**[4], **Torsten Rohlfing**[2], and **Adolf Pfefferbaum**[1,2]

[1]Department of Psychiatry & Behavioral Sciences, Stanford University School of Medicine, Stanford, CA

[2]Neuroscience Program, SRI International, Menlo Park, CA

[3]Applied Science Laboratory, GE Healthcare, Menlo Park, CA

[4]Department of Radiology Beth Israel Deaconess Medical Center, Boston, MA and Harvard University Medical School, Boston, MA

Abstract

Background—Alcoholism can disrupt neural synchrony between nodes of intrinsic functional networks that are maximally active when resting relative to engaging in a task, the default mode network (DMN) pattern. Untested, however, are whether the DMN in alcoholics can rebound normally from the relatively depressed task-state to the active resting-state and whether local perfusion deficits could disrupt network synchrony when switching from conditions of rest to task to rest, thereby indicating a physiological mechanism of neural network adaptation capability.

Methods—Whole-brain, 3D pulsed-continuous arterial spin labeling (PCASL) provided measurements of regional cerebral blood flow (rCBF) in 12 alcoholics and 12 controls under three conditions: pre-task rest, spatial working-memory task, post-task rest.

Results—With practice, alcoholics and controls achieved similar task accuracy and reaction times. Both groups exhibited a high-low-high pattern of perfusion levels in DMN regions during the rest-task-rest runs and the opposite pattern in posterior and cerebellar regions known to be associated with spatial working memory. Alcoholics showed selective differences from controls in the rest-task-rest CBF pattern in the anterior precuneus and CBF level in the insula, a hub of the salience network. Connectivity analysis identified activation synchrony from an insula seed to salience nodes (parietal, medial frontal, anterior cingulate cortices) in controls only.

Conclusions—We propose that attenuated insular CBF is a mechanism underlying compromised connectivity among salience network nodes. This local perfusion deficit in

[*]**Correspondence**, Edith V. Sullivan, Ph.D, Department of Psychiatry and Behavioral Sciences, Stanford University School of Medicine (MC5723), 401 Quarry Road, Stanford, CA 94305-5723, phone: (650) 859-2880, FAX: (650) 859-2743, edie@stanford.edu.

FINANCIAL DISCLOSURES

Drs. Pfefferbaum, Chanraud, Pitel, Müller-Oehring, Rohlfing, and Sullivan report no biomedical financial interests or potential conflicts of interest..

alcoholics has the potential to impair ability to switch from cognitive states of interoceptive cravings to cognitive control for curbing internal urges.

Keywords

arterial spin labeling; MRI; alcohol; working memory; perfusion; brain; connectivity

Introduction

Early neuroimaging studies on the effect of chronic alcoholism on brain function based on single photon emission computed tomography (SPECT) provided initial understanding of cerebral perfusion effects of alcohol dependence and change with sobriety. During alcohol withdrawal, regional cerebral blood flow (rCBF) relative to controls was abnormally low throughout the cortex, but particularly in frontal (1–4), temporal (3, 5–7), and cerebellar (8–10) regions, even without evidence of structural abnormalities (11). Recovery can accompany prolonged sobriety (1, 3). Studies using positron emission tomography (PET) with fluorodeoxyglucose (FDG) have yielded analogous results to those with SPECT, where sober alcoholics showed deficits in regional glucose metabolism early in abstinence and at least partial recovery with sustained abstinence (12–14). Even with sustained abstinence, low glucose metabolism persisted in frontal cortex (15, 16) and limbic sites (17) in uncomplicated alcoholism, extending to the anterior vermis in cases of alcoholic cerebellar degeneration with ataxia (18). To the extent that the functional magnetic resonance imaging (fMRI) blood oxygenation level-dependent (BOLD) response is "dependent" on cerebrovascular perfusion, chronic alcoholism has the potential of disturbing neural functions and their measurement by virtue of regional cerebrovascular insufficiencies. Moreover, regional differences in perfusion may also underlie differences in patterns of neural connectivity.

Current concepts of regional neural network activity differentiate activation in response to a task from fluctuating activity while in wakeful rest (19). The latter is considered a manifestation of intrinsic functional networks (e.g., 20, 21, 22), the most notable being the "default mode network (DMN)" (23). Identification of intrinsic functional networks relies on detecting synchronous activity among constellations of brain regions, commonly under task-free, resting conditions. Constellations identified while in a resting state are considered to be intrinsically related, concurrently engaged, and functionally relevant for monitoring interoceptive status and possibly for readying attentional systems to respond to changes in the environment (24–29). Determination of intrinsic networks has been accomplished using functional imaging modalities that reflect regional neuronal activity through their sensitivity to local changes in blood oxygenation, detected with the fMRI BOLD response (26), or in glucose metabolism, detected with FDG PET (30–32). Given that these physiological measures and the selective neural functions they reflect depend on local cerebral perfusion, disease-related disturbance of perfusion may itself affect selective brain functions and influence measurement.

Arterial spin labeling (ASL) perfusion imaging is a noninvasive, magnetic resonance (MR) method for measuring CBF (33) that has close similarities with CBF measurement using O^{15} PET (30, 31) and Tc-99m-HMPAO SPECT (10). ASL image resolution enables quantification of rCBF and registration with high-resolution structural MR images for localization and determination of tissue type and quality underlying perfusion (cf., 34, 35). An advantage of ASL over other noninvasive perfusion imaging methods is that it yields an absolute measure and is stable and reliable over time (e.g., 30, 36, 37–42), thereby enhancing the utility of ASL in tracking changes in brain activation as regions respond to tasks or absence of tasks without the need for depending on a differential response (43–46).

These features make ASL especially useful for identifying intrinsic functional networks in a resting state and for independently measuring the change in regional brain activity from resting when later engaged in selective cognitive tasks (cf., 34, 41).

Previously, we used whole-brain, pulsed continuous ASL (PCASL) imaging (47) with high-resolution, parcellated structural MRI to quantify changes in rCBF during performance of a cognitive task involving spatial working memory and during rest blocks before and after the task (34). The rCBF levels in nodes of the DMN fluctuated with the blocks of rest-task-rest, with higher rCBF levels in posterior cingulate, posterior-inferior precuneus, and medial frontal cortices in the two rest conditions and lower levels in the task condition. The return to the high-activation, resting state perfusion indicated consistency in the measure and robustness of DMN activation to an intervening cognitive task resulting in temporarily lower perfusion in DMN nodes while engaged in the task. A connectivity analysis, with an *a priori* seed in the posterior cingulate cortex, produced deactivation connectivity patterns consistent with the DMN and activation connectivity anatomically consistent with engagement in visuospatial tasks. The degree to which low perfusion can account for compromised regional connectivity in alcoholics (48–54) has not been investigated.

Herein, we examined abstinent alcohol dependents and low-drinking controls with PCASL measurements of rCBF under rest and task conditions. We predicted that regions in the DMN would have higher CBF during rest than task conditions and thus be differentiated from task-activated regions. We also asked whether alcoholism would modify these patterns and questioned whether DMN-related activation could return to pre-task levels in alcoholics (cf., 34). Also considered was the role of other abuse/dependence on observed alcoholism effects because of the high incidence of cocaine comorbidity in this sample. Finally, we examined whether local perfusion deficits would disrupt synchrony between nodes of intrinsic functional networks when switching from rest to task and back to rest conditions.

Methods

Participants

The groups comprised 12 men because they met DSM-IV (55) criteria for alcohol dependence and 12 control men matched in age (mean of each group=46 years, range=38–54 years) and handedness (56); the alcoholics had, on average, fewer years of education (Table 1 and Supplement 1). Alcoholics were recruited per protocol (57) by referral from local outpatient alcohol and addiction treatment centers and flyers distributed at community events. Controls were newly recruited for this study by referral from patient participants, Internet posting, flyers, and word of mouth. Calibrated clinical psychologists and research nurses administered the Structured Clinical Interview for DSM-IV (55) to identify individuals who met criteria for alcohol dependence or abuse; exclude those who met lifetime criteria for schizophrenia or bipolar disorder; and confirm that prospective controls did not meet DSM-IV criteria for any Axis I disorder. Quantity of lifetime alcohol consumption and date of last drink were obtained by interview (58–60). All but one alcoholic had refrained from drinking for at least 31 days; the exception had not drunk for 1 day, showed no withdrawal signs, and had a breathalyzer measurement of 0. Of the 12 alcoholics, eight also met criteria for a lifetime history of Cocaine Dependence (median sobriety = 347 weeks); two had an additional lifetime diagnosis of Opioid Dependence; one had past history of Amphetamine Dependence. No control was ever a cigarette smoker; 9 alcoholics were current or past smokers. (Supplement 1 provides additional participant data.) All subjects gave written informed consent for study participation. Internal Review Boards of Stanford University School of Medicine and SRI International gave approval to conduct this study.

MR Imaging Acquisition

Data were collected in a single session on a General Electric (Waukesha, WI) 3T Signa Excite human whole-body system, equipped with a receive-only 8-channel array head coil and body transmit coil. All participants were required to refrain from smoking and drinking caffeinated beverages for at least 2 hours prior to imaging. Three runs of a whole-brain PCASL 3D perfusion sequence (PCASL) (47, 61) permitted quantification of rCBF during rest, a spatial working memory task (62), and a second rest run in this order. Subjects had eyes open in all three conditions (6:49min per condition). Structural MRI data were used for anatomical localization of perfusion. In addition to a 3-plane localizer and calibration series for the multi-channel head coil, the protocols included a T1-weighted Spoiled Gradient Recalled (SPGR) sequence and a dual-echo, fast spin-echo (FSE) sequence.

MR Image and Perfusion Analysis

Analysis details are presented in Supplement 1. For each subject and each condition, PCASL CBF data were aligned via a rigid-body registration (http://nitrc.org/projects/cmtk) with the gray matter probability map because the CBF signal is predominantly in gray matter. Anatomical locations were identified with 16-region parcellations (Figure S1 in Supplement 1) (34) from the SRI24 atlas (http://nitrc.org/projects/sri24) (63). Data were analyzed as raw CBF in ml/100cc of gray matter/min for each region and each condition. To account for across-subject differences in global CBF and to express the data in terms of effect size, each individual's data were normalized by dividing the CBF value of each voxel minus the mean of the whole brain CBF by the standard deviation of the whole brain CBF:

$$\text{normalized CBF} = [(\text{voxel CBF} - \text{whole brain mean CBF}) / \text{whole brain CBF SD})].$$

CBF images were reformatted into SRI24 atlas coordinate space for group-average displays.

Spatial Working Memory Task

The spatial working memory task (62, 64) had two memoranda load conditions: 3 and 6 items (see Supplement and Figure S2). Subjects memorized spatial memoranda and recalled spatial sequences after a retention interval, either without interference (control condition) or with interference (cognitive arithmetic task or motor tracking task).

Rest-Task-Rest rCBF Temporal Connectivity Analysis

A connectivity analysis (34) using the three conditions, Rest 1, Task, Rest 2, in lieu of a traditional functional time series was conducted with the “conn” toolbox (http://www.fil.ion.ucl.ac.uk/spm/ext/), implemented in the Statistical Parametric Mapping (SPM) 8 software (Wellcome Department of Imaging Neuroscience, London, UK). Seeded voxel correlations between the signal from a seed region and that at every other brain voxel provided seed-to-voxel connectivity estimations using the CBF from the three conditions (Rest 1, Task, Rest 2) as the temporal variable. The *a priori* seeds were insula, anterior precuneus, posterior precuneus, and superior cerebellum, selected from observed between-group differences and patterns in CBF fluctuation. The magnitude and extent of temporal connectivity within each group were thresholded using a combined extent and peak intensity threshold with false discovery rate (FDR) correction of $P_{FDR} < 0.05$ for the whole brain volume (65).

Statistical Analysis

Group-by-condition analyses of variance (ANOVA), based on normalized CBF data, tested for differences between groups (alcoholics, controls), conditions (Rest 1, Task, Rest 2), laterality (left, right), and their interactions. Where appropriate, Greenhouse-Geisser (GG) correction was used. Follow-up comparisons of significant ANOVA effects used t-tests

(P_{FDR} with =.05 required p=.0028). Similarly, ANOVAs were conducted for the spatial working memory test and its conditions (34). Relations between rCBF and performance and demographic variables were examined with Pearson correlations; family-wise Bonferroni adjustment with =.05 (two-tailed) determined statistical significance.

Results

Group Differences in Regional Perfusion

Analyses (two -group by three -condition ANOVAs; P_{FDR} with =.05 required p=.029 for condition) performed on bilateral, normalized rCBF revealed four activation patterns relating to the three acquisition conditions (Rest 1, Task, Rest 2). Supplement 1 presents the means±SD CBF for each bilateral region by group (Table S1) and ANOVA (control vs. alcoholic; Table S2). Followup ANOVAs (three group [controls/alcoholics/alcoholics +cocaine] -by- two condition) considered the effect of cocaine comorbidity on activation patterns (Table S3). Intraclass correlations indicated high correspondence between normalized rCBF values by alcoholism subgroup for each condition (Rest 1 ICC r=.94; Task ICC r=.95; Rest 2 ICC r=.92; Figure S3).

The **DMN pattern** (high activation for Rest 1, low during the Task, return to high activation for Rest 2) was present in medial frontal, temporal, anterior and posterior cingulate, and posterior precuneus cortices and the hippocampus/amygdala. For these regions, ANOVAs yielded significant condition effects (p=.0001 for all but posterior cingulate p=.0357) but neither group effects nor group-by-condition interactions (Figure 1). The DMN pattern held in the same regions in the 3-group ANOVAs considering alcoholism/cocaine comorbidity (Table S3 in Supplement 1).

The **task-activated pattern** (low activation for Rest 1, high during the Task, return to low activation for Rest 2), indicated by condition effects, occurred in parietal (p=.0285), middle precuneus (p=.0014), and calcarine (p=.0001) cortices, inferior and superior cerebellum (p=.0001), and showed a trend in the occipital cortex (p=.0334). Neither group effects nor group-by-condition interactions were present in these regions, and the pattern in the superior cerebellum did not differ between the hemispheres (Figure 2). The task-activated pattern held in the same regions in the ANOVAs considering alcoholism/cocaine comorbidity (Table S3 in Supplement 1).

The **alcoholism pattern**, indicated by lower rCBF with ANOVA group effects, was present in the insula (p=.0031) and modestly in caudate/putamen (p=.0258) and globus pallidus (p=.0359) (Figure 3). The insula also exhibited the DMN pattern (p=.0017) with no group-by-condition interaction (p=.7435). Although the 3-group ANOVA effects for caudate/putamen and globus pallidus were not significant, the alcoholism group and condition pattern for the insula endured (Table S3 in Supplement 1). Further ANOVAs involving pairs of groups confirmed these effects for controls vs. alcoholics (group p=.0143; condition p=.001) and controls vs. alcoholics/cocaine (group p=.0074; condition p=.0024) but not for the alcoholics vs. alcoholics/cocaine comparison (group p=.439; condition p=.227).

The **interaction pattern** of anterior precuneus CBF (p=.0029) indicated opposing activation patterns in the groups, with controls showing the task-activation pattern and alcoholics showing the DMN pattern (Figure 3). Neither the separate effects of group nor repeated measures were significant. The interaction pattern held for the anterior precuneus in alcoholism/cocaine comorbidity ANOVAs (Table S3 in Supplement 1).

Neither group nor condition effects nor their interaction were significant in CBF of the lateral frontal cortex, total precuneus, or thalamus whether or not with alcoholism/cocaine comorbidity.

Figure 4 presents normalized rCBF values for each rest condition plotted against the task condition for the control and alcoholic groups separately. Both groups exhibited similar gradations of CBF values across the regions, with the lowest values in the globus pallidus and the highest in the posterior cingulate cortex. The relative positions of rCBF were nearly overlapping across the two rest conditions, indicating a general return to rest perfusion levels after task engagement.

Performance on the Spatial Working Memory Task

After practice, the two groups exhibited the same performance pattern and levels for accuracy and reaction time in the spatial working memory test (Figure S3 in Supplement 1). Both groups achieved greater accuracy ($F(1,22)=15.537$, $p=.0007$ GG) and shorter reaction times ($F(1,22)=277.873$, $p=.0001$ GG) in the 3 than 6 memoranda condition. Similarly, accuracy was better ($F(2,44)=8.935$, $p=.0006$ GG) and reaction times shorter ($F(2,44)=6.308$, $p=.0052$ GG) without than with retention interval interference. The same pattern was forthcoming when cocaine comorbidity was considered.

Spearman rank order correlations tested whether rCBF was predictive of performance and focused on the most difficult condition, recalling 6 spatial locations following a retention interval filled with arithmetic problems. The strongest correlations were as follows: Within the alcoholics, greater accuracy correlated with higher insular perfusion in Rest 1 ($Rho=.78$, $p=.0097$). Within the controls, shorter reaction times correlated modestly with higher medial frontal perfusion in Rest 1 ($Rho=-.71$, $p=.0192$), Task ($Rho=-.76$, $p=.0122$), and Rest 2 ($Rho=-.56$, $p=.0635$).

Regional Volume Analysis and Relations with rCBF

We measured the volumes of cortical and allocortical gray matter and subcortical tissue substrates of the rCBF to address whether group differences in tissue volumes could account for group differences in perfusion. Because the total brain tissue + CSF supratentorial volume of the controls was 8.7% greater than that of the alcoholics ($p=.0263$), we expressed the regional volumes as ratios of supratentorial volume (Table S4 in Supplement 1). Comparison using t-tests indicated two group differences: the insula ratio tended to be smaller in the alcoholics than controls regardless of cocaine comorbidity ($p=.0668$); by contrast, the caudate/putamen ratio was larger than controls only in the alcoholics with cocaine comorbidity ($p=.0127$).

We next pursued the possible influence of regional volume ratios on CBF by using regional volumes as covariates in ANCOVAs to test group differences in rCBF. In no case did the ANCOVAs identifying group differences in rCBF yield results different from those obtained without consideration of the underlying tissue volume.

Correlates of Regional Perfusion

Individually normalized regional perfusion measures did not correlate significantly with age, lifetime alcohol consumption, years of education, or smoking status within either group or when the groups were combined. Despite higher incidence of smokers in alcoholics than controls, alcoholics had even higher (albeit not significantly) average native, non-normalized, whole-brain cortical gray matter CBF values than controls in all PCASL conditions. Further, neither non-normalized nor normalized rCBF levels differed between participants with (9 alcoholics) vs. those without (3 alcoholics + 12 controls) a history of

smoking. Similarly, when considering alcoholics only, smoking history did not differentiate the groups. Indeed, the only regions showing a trend (p=.079) toward a group difference was the insula at Rest 2, at which time the alcoholic smokers had higher perfusion than alcoholic non-smokers.

Synchrony of Regional Perfusion from Rest 1-to-Task-to-Rest 2

Synchrony of normalized regional perfusion across conditions was assessed using a seed-to-ROI approach. Given abnormally low CBF in the alcoholics' insula, we chose the left+right insula as the seed for whole-brain connectivity analysis (Figure 9). Within controls, rest-task-rest activation of the bilateral insula was synchronous with activity fluctuation in bilateral anterior cingulate, medial and lateral frontal, and insular cortices; left parietal lobe (including supramarginal gyrus); and right superior temporal gyrus (Table 4). For alcoholics, none of the insula-ROI connectivity tests met FDR correction. In no case did alcoholics show evidence for greater connectivity than controls, but the opposite did occur. Synchrony between the bilateral insular seed and the left parietal (extending to the supramarginal gyrus), medial frontal, and anterior cingulate cortices met FDR correction for significant differences, greater in the controls than alcoholics (Figure 5; Table S4 in Supplement 1). Additional analyses appear in Supplement 1.

Discussion

Like controls, the alcoholics exhibited the high-low-high pattern of regional perfusion levels in nodes of the DMN, notably the medial frontal, anterior and posterior cingulate, posterior precuneus, and lateral and medial temporal cortices during the rest-task-rest runs. All groups also exhibited the task-activated pattern, which was the inverse of the DMN pattern, in parietal, occipital, and cerebellar regions known to be associated with the spatial working memory task employed (62, 66). In contrast with the posterior DMN precuneus pattern and middle precuneus task-activation pattern, the groups differed in the rest-task-rest pattern of CBF activation in the anterior precuneus, where controls showed a task-activated pattern, whereas alcoholics (with or without cocaine history) showed the DMN/rest-activated pattern. These functional differences support the heterogeneity of the precuneus structurally (67) and functionally (34, 68). An additional group difference occurred in the CBF level in the insula, a brain region central to addiction circuitry and principal node of the salience network. Thus, depending on the region examined, CBF levels either returned to high or to low levels at Rest 2 from Rest 1 in alcoholics and controls. These patterns and activation levels could be established because PCASL enabled independent measurement of rCBF without relying on differential signals to detect resting state and task-activated patterns (cf., 46, 69).

Despite the common DMN pattern exhibited by the groups across conditions, the mean activation level across conditions in the insula of the alcoholics was only 61% (50.3% for alcoholics; 66.5% for comorbids) of that of the controls. This locally depressed CBF probably contributed to the alcoholics' connectivity "deficit" identified when testing for regions of synchronous activity with the insula seed. In contrast with alcoholics, who showed no significant insular connectivity, controls produced robust synchrony between the insula and DMN and executive control network nodes, including the anterior cingulate, medial frontal and parietal cortices (23, 26, 70). Functional synchrony among these brain regions is consistent with connectivity marking the salience network and communication between the salience network (incorporating the insula, medial frontal, anterior cingulate, and dorsolateral prefrontal cortices and thalamus) and the executive control network (incorporating the dorsolateral prefrontal, orbitofrontal superior parietal cortices including the angular and supramarginal gyri) (22).

Although enigmatic for decades, functions of the insula are now being revealed. Functions invoking insular activity involve impulse control (71), self-regulation (72), conscious perception of error monitoring (73), awareness of salience (74), and reward processing (75, 76). In its role as directing interoceptive experiences of pleasure and craving, the insula has been hypothesized to be central in decision making about consuming drugs (including cocaine (77, 78)) and alcohol (79) and linked to stress in "addiction circuitry" (80). Impulse control measured in alcoholics while engaged in a Stop Signal paradigm revealed that poorer impulse control was related to lower activity in regions of the salience network including the insula (71). Such poor impulse control might be explained, at least in part, by impaired insular perfusion, as observed herein, impairing the potential for demonstrating perfusion-based functional connections.

CBF levels of the insula were at similar levels in the groups relative to the other brain regions measured (Figure 4). Nonetheless, the insula had a significant perfusion deficit in the alcoholics regardless of cocaine history, which may have diminished the insula's normal capacity to serve as a hub with critical nodes of the salience, executive control, and default mode networks. Indeed, a central process of the salience network is thought to enable switching between resting and activation states within networks with common nodes or between brain networks (28, 81). The switch could be from interoceptive processing of DMN to exteroceptive awareness of the executive control network to heed environmental demands and attend to imperative stimuli (cf., 22, 28). Areas that showed synchrony with the insula in the controls were the parietal cortex (including the left supramarginal gyrus purported to be involved in reward regulation), dorsolateral prefrontal cortex (a node of the executive control network), and anterior cingulate cortex (a common node of the salience and executive control networks). These areas, however, were poorly synchronized in alcoholics, suggesting a functional mechanism for impaired ability to switch between networks and access executive control processes to regulate behavior.

In contrast with the failure to synchronize nodes of the salience network, the alcoholics showed greater connectivity than controls between the superior cerebellar seed and nodes of the salience network, excluding the insula but including the lateral and medial frontal, temporal, and parietal cortices extending to the right angular and fusiform gyri. This positive connectivity in the alcoholics may appear paradoxical given that the rest-task-rest CBF pattern of the cerebellum showed the opposite pattern to that of the insula. This cerebellar-based synchrony might be interpreted to serve a compensatory connectivity function to alcoholics, whose insular-based switching mechanism of the salience network is compromised. Although support for cerebellar-based network compensation has precedent in alcoholism (66), this speculation requires direct experimentation.

Three earlier studies used single-slice ASL to measure CBF in alcoholism. Young alcohol dependent women exhibited modestly lower perfusion in the prefrontal and left parietal cortical regions (82). Alcoholics, particularly smokers, had lower perfusion in frontal and parietal gray matter than controls (83). One longitudinal study revealed CBF improvement in alcoholics after 5 weeks of sobriety relative to their baseline at 1 week, but only nonsmoking alcoholics showed substantial improvement (84). Despite the high incidence of smokers in our alcoholics, history of smoking was not related to CBF abnormalities. Rather, absolute CBF measurement revealed consistently high rates in both controls and alcoholics (with and without a smoking history) in the principal DMN nodes compared with other brain regions.

Among the study's many limitations are small sample size, history of multiple drug use in some alcoholics, examination of men only, widely varying lengths of sobriety, polydrug use (increasingly common), and restricted age range. Comorbid history of cocaine in the

majority of the alcoholics is another potentially confounding factor given reports of cocaine-related volume (85, 86) and density (87) deficits in prefrontal cortex and focal volume deficits in orbitofrontal (77, 78, 88) and insular (77, 89) cortices. CBF measured with SPECT is also depressed in cocaine addiction but is selective to orbitofrontal and superior temporal cortices (78), regions not implicated in the rCBF patterns noted in the present study.

Previously, we speculated that disease-related diminution of a rebound in CBF from evoked (task) to intrinsic (resting) activity levels might represent impairment in functional readiness or neural reserve (34). Consistent with this possibility, Raichle (90) anticipated that "the strength of coherence between nodes within systems varies with age and disease" (page 4). Rather than globally dampened CBF, we observed selective regions of abnormal perfusion levels in the insula and opposite rest-task-rest patterns in the anterior precuneus in the alcoholics and controls. We now propose that 1) dampened insular CBF may be a mechanism accounting for the attenuated neural activity identified in task-activated studies based on a differential BOLD response; and 2) abnormal CBF levels in the insula indicate a physiological mechanism that underlies compromised connectivity among nodes of the salience network and reduces ability to switch from introspection and interoceptive desires and cravings to cognitive control over these urges.

Supplementary Material

Refer to Web version on PubMed Central for supplementary material.

Acknowledgments

We would like to extend special thanks to Stephanie A. Sassoon, Ph.D. for diagnostic oversight of the study participants. This work was supported by NIH grants AA012388, AA010723, AA017347, AA017168, AA017923, EB008381, MH80729.

Dr. Shankaranarayanan is an employee of General Electric Healthcare, the manufacturer of the MR system used in this study. Dr. Alsop is an inventor on patents related to the arterial spin labeling protocols used herein and may receive patent-related royalties; he also receives research support from GE Healthcare.

REFERENCES

1. Nicolas JM, Catafau AM, Estruch R, Lomena FJ, Salamero M, Herranz R, et al. Regional cerebral blood Flow-SPECT in chronic alcoholism: Relation to neuropsychological testing. J Nucl Med. 1993; 34:1452–1459. [PubMed: 8355063]
2. Kuruoglu AC, Arikan Z, Vural G, Karatas M, Arac M, Isik E. Single photon emission computerised tomography in chronic alcoholism - antisocial personality disorder may be associated with decreased frontal perfusion. Br J Psychiatry. 1996; 169:348–354. [PubMed: 8879722]
3. Tutus A, Kugu N, Sofuoglu S, Nardali M, Simsek A, Karaaslan F, et al. Transient frontal hypoperfusion in Tc-99m hexamethylpropyleneamineoxime single photon emission computed tomography imaging during alcohol withdrawal. Biol Psychiatry. 1998; 43:923–928. [PubMed: 9627750]
4. Gansler DA, Harris GJ, Oscar-Berman M, Streeter C, Lewis RF, Ahmed I, et al. Hypoperfusion of inferior frontal brain regions in abstinent alcoholics: a pilot SPECT study. Journal of Studies on Alcoholism. 2000; 61:32–37.
5. Caspari D, Trabert W, Heinz G, Lion N, Henkes H, Huber G. The pattern of regional cerebral blood flow during alcohol withdrawal--a single photon emission tomography study with 99mTc-HMPAO. Acta Psychiatr Scand. 1993; 87:414–417. [PubMed: 8356893]
6. George MS, Teneback CC, Malcolm RJ, Moore J, Stallings LE, Spicer KM, et al. Multiple previous alcohol detoxifications are associated with decreased medial temporal and paralimbic function in the postwithdrawal period. Alcohol Clin Exp Res. 1999; 23:1077–1084. [PubMed: 10397294]

7. Suzuki Y, Oishi M, Ogawa K, Mizutani T. Atrophy of the parahippocampal gyrus and regional cerebral blood flow in the limbic system in chronic alcoholic patients. Alcohol. 2010; 44:439–445. [PubMed: 20804943]
8. Jordaan GP, Warwick JM, Hewlett R, Emsley R. Resting brain perfusion in alcohol-induced psychotic disorder: a comparison in patients with alcohol dependence, schizophrenia and healthy controls. Prog Neuropsychopharmacol Biol Psychiatry. 2010; 34:479–485. [PubMed: 20122978]
9. Harris GJ, Oscar-Berman M, Gansler A, Streeter C, Lewis RF, Ahmed I, et al. Hypoperfusion of the cerebellum and aging effects on cerebral cortex blood flow in abstinent alcoholics: a SPECT study. Alcoholism, clinical and experimental research. 1999; 23:1219–1227.
10. Demir B, Ulug B, Lay Ergun E, Erbas B. Regional cerebral blood flow and neuropsychological functioning in early and late onset alcoholism. Psychiatry Res. 2002; 115:115–125. [PubMed: 12208489]
11. Melgaard B, Henriksen L, Ahlgren P, Danielsen UT, Sorensen H, Paulson OB. Regional cerebral blood flow in chronic alcoholics measured by single photon emission computerized tomography. Acta Neurol Scand. 1990; 82:87–93. [PubMed: 2256449]
12. Fellgiebel A, Scheurich A, Siessmeier T, Schmidt LG, Bartenstein P. Persistence of disturbed thalamic glucose metabolism in a case of Wernicke-Korsakoff syndrome. Psychiatry Res. 2003; 124:105–112. [PubMed: 14561428]
13. Johnson-Greene D, Adams KM, Gilman S, Kluin KJ, Junck L, Martorello S, et al. Impaired upper limb coordination in alcoholic cerebellar degeneration. Arch Neurol. 1997; 54:436–439. [PubMed: 9109745]
14. Asada T, Takaya S, Takayama Y, Yamauchi H, Hashikawa K, Fukuyama H. Reversible alcohol-related dementia: a five-year follow-up study using FDG-PET and neuropsychological tests. Intern Med. 2010; 49:283–287. [PubMed: 20154432]
15. Wang GJ, Volkow ND, Roque CT, Cestaro VL, Hitzemann RJ, Cantos EL, et al. Functional importance of ventricular enlargement and cortical atrophy in healthy subjects and alcoholics as assessed with PET, MR imaging, and neuropsychologic testing. Radiology. 1993; 186:59–65. [PubMed: 8416587]
16. Adams KM, Gilman S, Koeppe RA, Kluin KJ, Brunberg JA, Dede D, et al. Neuropsychological deficits are correlated with frontal hypometabolism in positron emission tomography studies of older alcoholic patients. Alcoholism: Clinical and Experimental Research. 1993; 17:205–210.
17. Wik G, Borg S, Sjögren I, Wiesel FA, Blomqvist G, Borg J, et al. PET determination of regional cerebral glucose metabolism in alcohol-dependent men and healthy controls using ^{11}C-glucose. Acta Psychiatr Scand. 1988; 78:234–241. [PubMed: 2851920]
18. Gilman S, Adams K, Koeppe RA, Berent S, Kluin KJ, Modell JG, et al. Cerebellar and frontal hypometabolism in alcoholic cerebellar degeneration studied with Positron Emission Tomography. Ann Neurol. 1990; 28:775–785. [PubMed: 2285264]
19. Biswal B, Yetkin FZ, Haughton VM, Hyde JS. Functional connectivity in the motor cortex of resting human brain using echo-planar MRI. Magn Reson Med. 1995; 34:537–541. [PubMed: 8524021]
20. Tomasi D, Volkow ND. Association between functional connectivity hubs and brain networks. Cereb Cortex. 2011; 21:2003–2013. [PubMed: 21282318]
21. Habas C, Kamdar N, Nguyen D, Prater K, Beckmann CF, Menon V, et al. Distinct cerebellar contributions to intrinsic connectivity networks. J Neurosci. 2009; 29:8586–8594. [PubMed: 19571149]
22. Seeley WW, Menon V, Schatzberg AF, Keller J, Glover GH, Kenna H, et al. Dissociable intrinsic connectivity networks for salience processing and executive control. J Neurosci. 2007; 27:2349–2356. [PubMed: 17329432]
23. Raichle M, MacLeod A, Snyder A, Powers W, Gusnard D, Shulman G. A default mode of brain function. Proc Natl Acad Sci U S A. 2001; 98:676–682. [PubMed: 11209064]
24. Vincent JL, Snyder AZ, Fox MD, Shannon BJ, Andrews JR, Raichle ME, et al. Coherent spontaneous activity identifies a hippocampal-parietal memory network. J Neurophysiol. 2006; 96:3517–3531. [PubMed: 16899645]

25. Buckner RL, Andrews-Hanna JR, Schacter DL. The brain's default network: anatomy, function, and relevance to disease. Annals of the New York Academy of Sciences. 2008; 1124:1–38. [PubMed: 18400922]
26. Greicius MD, Krasnow B, Reiss AL, Menon V. Functional connectivity in the resting brain: a network analysis of the default mode hypothesis. Proc Natl Acad Sci U S A. 2003; 100:253–258. [PubMed: 12506194]
27. Fox MD, Snyder AZ, Vincent JL, Corbetta M, Van Essen DC, Raichle ME. The human brain is intrinsically organized into dynamic, anticorrelated functional networks. Proc Natl Acad Sci U S A. 2005; 102:9673–9678. [PubMed: 15976020]
28. Sridharan D, Levitin DJ, Menon V. A critical role for the right fronto-insular cortex in switching between central-executive and default-mode networks. Proc Natl Acad Sci U S A. 2008; 105:12569–12574. [PubMed: 18723676]
29. Raichle ME, Gusnard DA. Intrinsic brain activity sets the stage for expression of motivated behavior. J Comp Neurol. 2005; 493:167–176. [PubMed: 16254998]
30. Xu G, Rowley HA, Wu G, Alsop DC, Shankaranarayanan A, Dowling M, et al. Reliability and precision of pseudo-continuous arterial spin labeling perfusion MRI on 3.0 T and comparison with 15O-water PET in elderly subjects at risk for Alzheimer's disease. NMR Biomed. 2010; 23:286–293. [PubMed: 19953503]
31. Ye FQ, Berman KF, Ellmore T, Esposito G, van Horn JD, Yang Y, et al. H(2)(15)O PET validation of steady-state arterial spin tagging cerebral blood flow measurements in humans. Magn Reson Med. 2000; 44:450–456. [PubMed: 10975898]
32. Raichle ME, Snyder AZ. A default mode of brain function: a brief history of an evolving idea. NeuroImage. 2007; 37:1083–1090. discussion 1097–1089. [PubMed: 17719799]
33. Detre JA, Leigh JS, Williams DS, Koretsky AP. Perfusion imaging. Magn Reson Med. 1992; 23:37–45. [PubMed: 1734182]
34. Pfefferbaum A, Chanraud S, Pitel A-L, Müller-Oehring EM, Shankaranarayanan A, Alsop D, et al. Cerebral blood flow in posterior cortical nodes of the default mode network decreases with task engagement but remains higher than in most brain regions. Cereb Cortex. 2011; 21:233–244. [PubMed: 20484322]
35. Alsop DC, Dai W, Grossman M, Detre JA. Arterial spin labeling blood flow MRI: its role in the early characterization of Alzheimer's disease. J Alzheimers Dis. 2010; 20:871–880. [PubMed: 20413865]
36. Wang J, Aguirre GK, Kimberg DY, Roc AC, Li L, Detre JA. Arterial spin labeling perfusion fMRI with very low task frequency. Magn Reson Med. 2003; 49:796–802. [PubMed: 12704760]
37. MacIntosh BJ, Pattinson KT, Gallichan D, Ahmad I, Miller KL, Feinberg DA, et al. Measuring the effects of remifentanil on cerebral blood flow and arterial arrival time using 3D GRASE MRI with pulsed arterial spin labelling. J Cereb Blood Flow Metab. 2008; 28:1514–1522. [PubMed: 18506198]
38. Aguirre GK, Detre JA, Zarahn E, Alsop DC. Experimental design and the relative sensitivity of BOLD and perfusion fMRI. Neuroimage. 2002; 15:488–500. [PubMed: 11848692]
39. Parkes LM, Rashid W, Chard DT, Tofts PS. Normal cerebral perfusion measurements using arterial spin labeling: reproducibility, stability, and age and gender effects. Magn Reson Med. 2004; 51:736–743. [PubMed: 15065246]
40. Petersen ET, Mouridsen K, Golay X. The QUASAR reproducibility study, Part II: Results from a multi-center Arterial Spin Labeling test-retest study. Neuroimage. 2010; 49:104–113. [PubMed: 19660557]
41. Pfefferbaum A, Chanraud S, Pitel A-L, Shankaranarayanan A, Alsop DC, Rohlfing T, et al. Volumetric cerebral perfusion imaging in healthy adults: Regional distribution, laterality, and repeatability of pulsed continuous arterial spin labeling (PCASL). Psychiatry Research: Neuroimaging. 2010; 182:266–273.
42. Floyd TF, Ratcliffe SJ, Wang J, Resch B, Detre JA. Precision of the CASL-perfusion MRI technique for the measurement of cerebral blood flow in whole brain and vascular territories. J Magn Reson Imaging. 2003; 18:649–655. [PubMed: 14635149]

43. Gusnard DA, Akbudak E, Shulman GL, Raichle ME. Medial prefrontal cortex and self-referential mental activity: relation to a default mode of brain function. Proc Natl Acad Sci U S A. 2001; 98:4259–4264. [PubMed: 11259662]
44. Wong EC, Buxton RB, Frank LR. A theoretical and experimental comparison of continuous and pulsed arterial spin labeling techniques for quantitative perfusion imaging. Magn Reson Med. 1998; 40:348–355. [PubMed: 9727936]
45. Buxton RB, Wong EC, Frank LR. Dynamics of blood flow and oxygenation changes during brain activation: the balloon model. Magn Reson Med. 1998; 39:855–864. [PubMed: 9621908]
46. Detre JA, Wang J, Wang Z, Rao H. Arterial spin-labeled perfusion MRI in basic and clinical neuroscience. Curr Opin Neurol. 2009; 22:348–355. [PubMed: 19491678]
47. Dai W, Garcia D, de Bazelaire C, Alsop DC. Continuous flow-driven inversion for arterial spin labeling using pulsed radio frequency and gradient fields. Magn Reson Med. 2008; 60:1488–1497. [PubMed: 19025913]
48. Camchong J, Stenger A, Fein G. Resting-State Synchrony During Early Alcohol Abstinence Can Predict Subsequent Relapse. Cereb Cortex. 2012
49. Camchong J, Stenger A, Fein G. Resting-State Synchrony in Long-Term Abstinent Alcoholics. Alcoholism, clinical and experimental research. 2012
50. Pitel AL, Chanraud S, Rohlfing T, Pfefferbaum A, Sullivan EV. Face-name association learning and brain structural substrates in alcoholism. Alcoholism: Clinical and Experimental Research. 2012 epub 2012 Apr 2017.
51. Schulte T, Müller-Oehring EM, Sullivan EV, Pfefferbaum A. Synchrony of corticostriatal-midbrain activation enables normal inhibitory control and conflict processing in recovering alcoholic men. Biological Psychiatry. 2012; 17:269–278. [PubMed: 22137506]
52. Kim E, Ku J, Namkoong K, Lee W, Lee KS, Park JY, et al. Mammillothalamic functional connectivity and memory function in Wernicke's encephalopathy. Brain. 2009; 132:369–376. [PubMed: 19036763]
53. O'Daly OG, Trick L, Scaife J, Marshall J, Ball D, Phillips ML, et al. Withdrawal-associated increases and decreases in functional neural connectivity associated with altered emotional regulation in alcoholism. Neuropsychopharmacology. 2012; 37:2267–2276. [PubMed: 22617355]
54. Rogers BP, Parks MH, Nickel MK, Katwal SB, Martin PR. Reduced fronto-cerebellar functional connectivity in chronic alcoholic patients. Alcoholism, clinical and experimental research. 2012; 36:294–301.
55. First, MB.; Spitzer, RL.; Gibbon, M.; Williams, JBW. Structured Clinical Interview for DSM-IV Axis I Disorders (SCID) Version 2.0. New York, NY: Biometrics Research Department, New York State Psychiatric Institute; 1998.
56. Crovitz HF, Zener KA. Group test for assessing hand and eye dominance. Am J Psychol. 1962; 75:271–276. [PubMed: 13882420]
57. Pfefferbaum A, Rosenbloom MJ, Rohlfing T, Adalsteinsson E, Kemper CA, Deresinski S, et al. Contribution of alcoholism to brain dysmorphology in HIV infection: Effects on the ventricles and corpus callosum. Neuroimage. 2006; 33:239–251. [PubMed: 16877010]
58. Skinner, HA. Development and Validation of a Lifetime Alcohol Consumption Assessment Procedure. Toronto, Canada: Addiction Research Foundation; 1982.
59. Skinner HA, Sheu WJ. Reliability of alcohol use indices: The lifetime drinking history and the MAST. J Stud Alcohol. 1982; 43:1157–1170. [PubMed: 7182675]
60. Pfefferbaum A, Lim KO, Zipursky RB, Mathalon DH, Rosenbloom MJ, Lane B, et al. Brain gray and white matter volume loss accelerates with aging in chronic alcoholics: A quantitative MRI study. Alcoholism: Clinical and Experimental Research. 1992; 16:1078–1089.
61. Dai W, PM R, Shankaranarayanan A, Alsop DC. ASL Perfusion Measurement Using a Rapid, Low Resolution Arterial Transit Time Prescan. Proceedings of the 17th International Society of Magnetic Resonance in Medicine. 2009:3585.
62. Chanraud S, Pitel AL, Pfefferbaum A, Sullivan EV. Disruption of functional connectivity of the default-mode network in alcoholism. Cereb Cortex. 2011; 10:2272–2281. [PubMed: 21368086]
63. Rohlfing T, Zahr NM, Sullivan EV, Pfefferbaum A. The SRI24 multi-channel atlas of normal adult human brain structure. Hum Brain Mapp. 2010; 31:798–819. [PubMed: 20017133]

64. Chanraud S, Pitel A-L, Rohlfing T, Pfefferbaum A, Sullivan EV. Dual tasking and working memory in alcoholism: Relation to frontocerebellar circuitry. Neuropsychopharmacology. 2010; 35:1868–1878. [PubMed: 20410871]
65. Poline JB, Worsley KJ, Evans AC, Friston KJ. Combining spatial extent and peak intensity to test for activations in functional imaging. NeuroImage. 1997; 5:83–96. [PubMed: 9345540]
66. Chanraud S, Pitel AL, Müller-Oehring EM, Pfefferbaum A, Sullivan EV. Remapping the brain to compensate for impairment in recovering alcoholics. Cereb Cortex. 2012 in press.
67. Margulies DS, Vincent JL, Kelly C, Lohmann G, Uddin LQ, Biswal BB, et al. Precuneus shares intrinsic functional architecture in humans and monkeys. Proc Natl Acad Sci U S A. 2009; 106:20069–20074. [PubMed: 19903877]
68. Zhang S, Li CS. Functional connectivity mapping of the human precuneus by resting state fMRI. NeuroImage. 59:3548–3562. [PubMed: 22116037]
69. Khalili-Mahani N, van Osch MJ, Baerends E, Soeter RP, de Kam M, Zoethout RW, et al. Pseudocontinuous arterial spin labeling reveals dissociable effects of morphine and alcohol on regional cerebral blood flow. J Cereb Blood Flow Metab. 2011; 31:1321–1333. [PubMed: 21245872]
70. Greicius MD, Supekar K, Menon V, Dougherty RF. Resting-state functional connectivity reflects structural connectivity in the default mode network. Cereb Cortex. 2009; 19:72–78. [PubMed: 18403396]
71. Li CS, Luo X, Yan P, Bergquist K, Sinha R. Altered impulse control in alcohol dependence: neural measures of stop signal performance. Alcoholism, clinical and experimental research. 2009; 33:740–750.
72. Ansell EB, Rando K, Tuit K, Guarnaccia J, Sinha R. Cumulative adversity and smaller gray matter volume in medial prefrontal, anterior cingulate, and insula regions. Biol Psychiatry. 2012; 72:57–64. [PubMed: 22218286]
73. Ullsperger M, Harsay HA, Wessel JR, Ridderinkhof KR. Conscious perception of errors and its relation to the anterior insula. Brain Struct Funct. 2010; 214:629–643. [PubMed: 20512371]
74. Craig AD. How do you feel? Interoception: the sense of the physiological condition of the body. Nat Rev Neurosci. 2002; 3:655–666. [PubMed: 12154366]
75. Koob GF, Kenneth Lloyd G, Mason BJ. Development of pharmacotherapies for drug addiction: a Rosetta stone approach. Nat Rev Drug Discov. 2009; 8:500–515. [PubMed: 19483710]
76. Koob GF. Neurobiological substrates for the dark side of compulsivity in addiction. Neuropharmacology. 2009; 56(Suppl 1):18–31. [PubMed: 18725236]
77. Ersche KD, Barnes A, Jones PS, Morein-Zamir S, Robbins TW, Bullmore ET. Abnormal structure of frontostriatal brain systems is associated with aspects of impulsivity and compulsivity in cocaine dependence. Brain. 2011; 134:2013–2024. [PubMed: 21690575]
78. Adinoff B, Braud J, Devous MD, Harris TS. Caudolateral orbitofrontal regional cerebral blood flow is decreased in abstinent cocaine-addicted subjects in two separate cohorts. Addict Biol. 2011; 17:1001–1012. [PubMed: 22129494]
79. Naqvi NH, Bechara A. The insula and drug addiction: an interoceptive view of pleasure, urges, and decision-making. Brain Struct Funct. 2010; 214:435–450. [PubMed: 20512364]
80. Koob GF, Volkow ND. Neurocircuitry of addiction. Neuropsychopharmacology. 2010; 35:217–238. [PubMed: 19710631]
81. Menon V, Uddin LQ. Saliency, switching, attention and control: a network model of insula function. Brain Struct Funct. 2010; 214:655–667. [PubMed: 20512370]
82. Clark CP, Brown GG, Eyler LT, Drummond SP, Braun DR, Tapert SF. Decreased perfusion in young alcohol-dependent women as compared with age-matched controls. Am J Drug Alcohol Abuse. 2007; 33:13–19. [PubMed: 17366242]
83. Gazdzinski S, Durazzo T, Jahng GH, Ezekiel F, Banys P, Meyerhoff D. Effects of chronic alcohol dependence and chronic cigarette smoking on cerebral perfusion: a preliminary magnetic resonance study. Alcoholism: Clinical and Experimental Research. 2006; 30:947–958.
84. Mon A, Durazzo TC, Gazdzinski S, Meyerhoff DJ. The Impact of Chronic Cigarette Smoking on Recovery From Cortical Gray Matter Perfusion Deficits in Alcohol Dependence: Longitudinal Arterial Spin Labeling MRI. Alcohol Clin Exp Res. 2009; 33:1314–1321. [PubMed: 19413652]

85. Fein G, Di Sclafani V, Meyerhoff D. Prefrontal cortical volume reduction associated with frontal cortex function deficit in 6-week abstinent crack-cocaine dependent men. Drug Alcohol Depend. 2002; 68:87–93. [PubMed: 12167554]

86. O'Neill J, Cardenas VA, Meyerhoff DJ. Separate and interactive effects of cocaine and alcohol dependence on brain structures and metabolites: quantitative MRI and proton MR spectroscopic imaging. Addict Biol. 2001; 6:347–361. [PubMed: 11900613]

87. Matochik JA, London ED, Eldreth DA, Cadet JL, Bolla KI. Frontal cortical tissue composition in abstinent cocaine abusers: a magnetic resonance imaging study. NeuroImage. 2003; 19:1095–1102. [PubMed: 12880835]

88. Tanabe J, Tregellas JR, Dalwani M, Thompson L, Owens E, Crowley T, et al. Medial orbitofrontal cortex gray matter is reduced in abstinent substance-dependent individuals. Biol Psychiatry. 2009; 65:160–164. [PubMed: 18801475]

89. Franklin TR, Acton PD, Maldjian JA, Gray JD, Croft JR, Dackis CA, et al. Decreased gray matter concentration in the insular, orbitofrontal, cingulate, and temporal cortices of cocaine patients. Biol Psychiatry. 2002; 51:134–142. [PubMed: 11822992]

90. Raichle ME. The restless brain. Brain Connect. 2011; 1:3–12. [PubMed: 22432951]

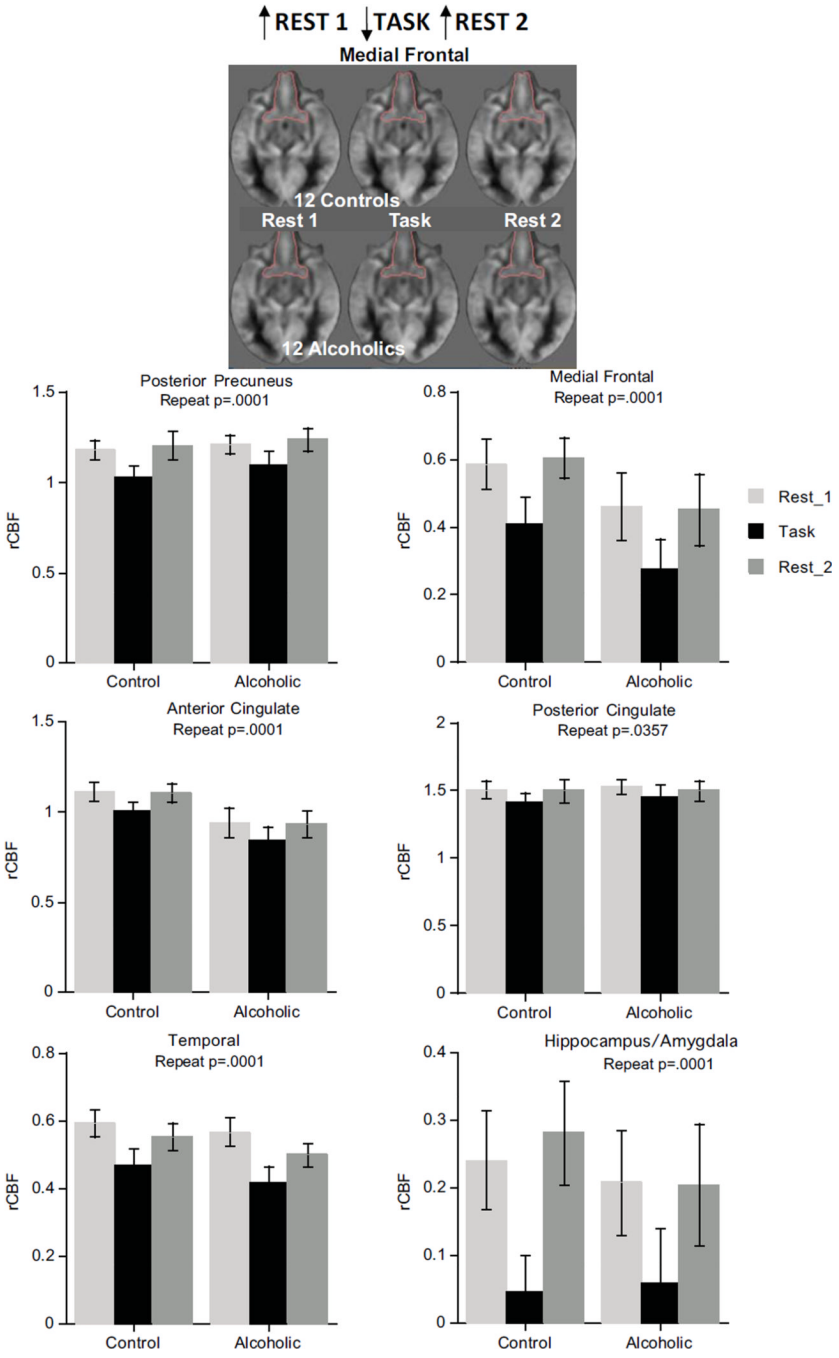

Figure 1.
Brain regions showing DMN pattern.

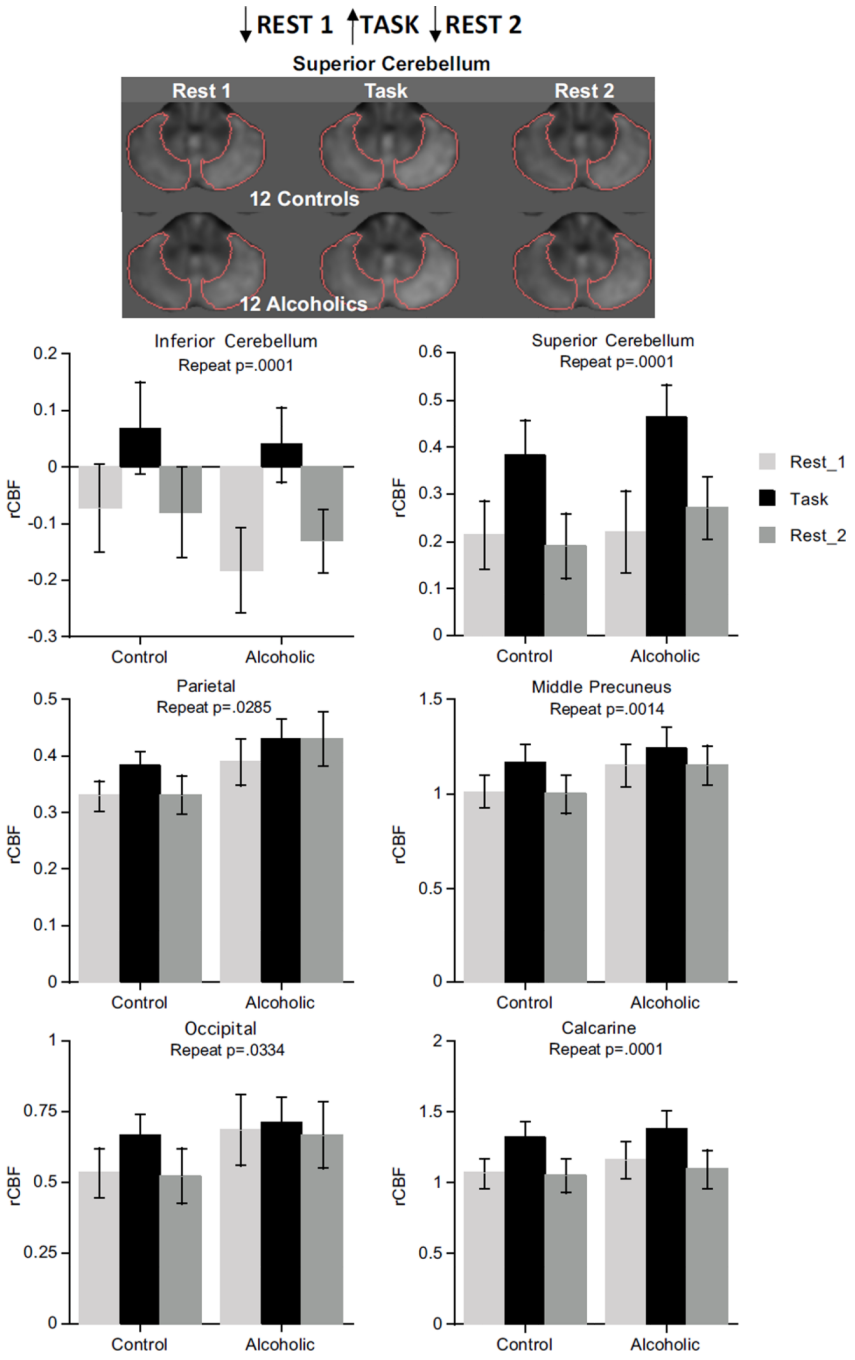

Figure 2.
Brain regions showing task-activated pattern.

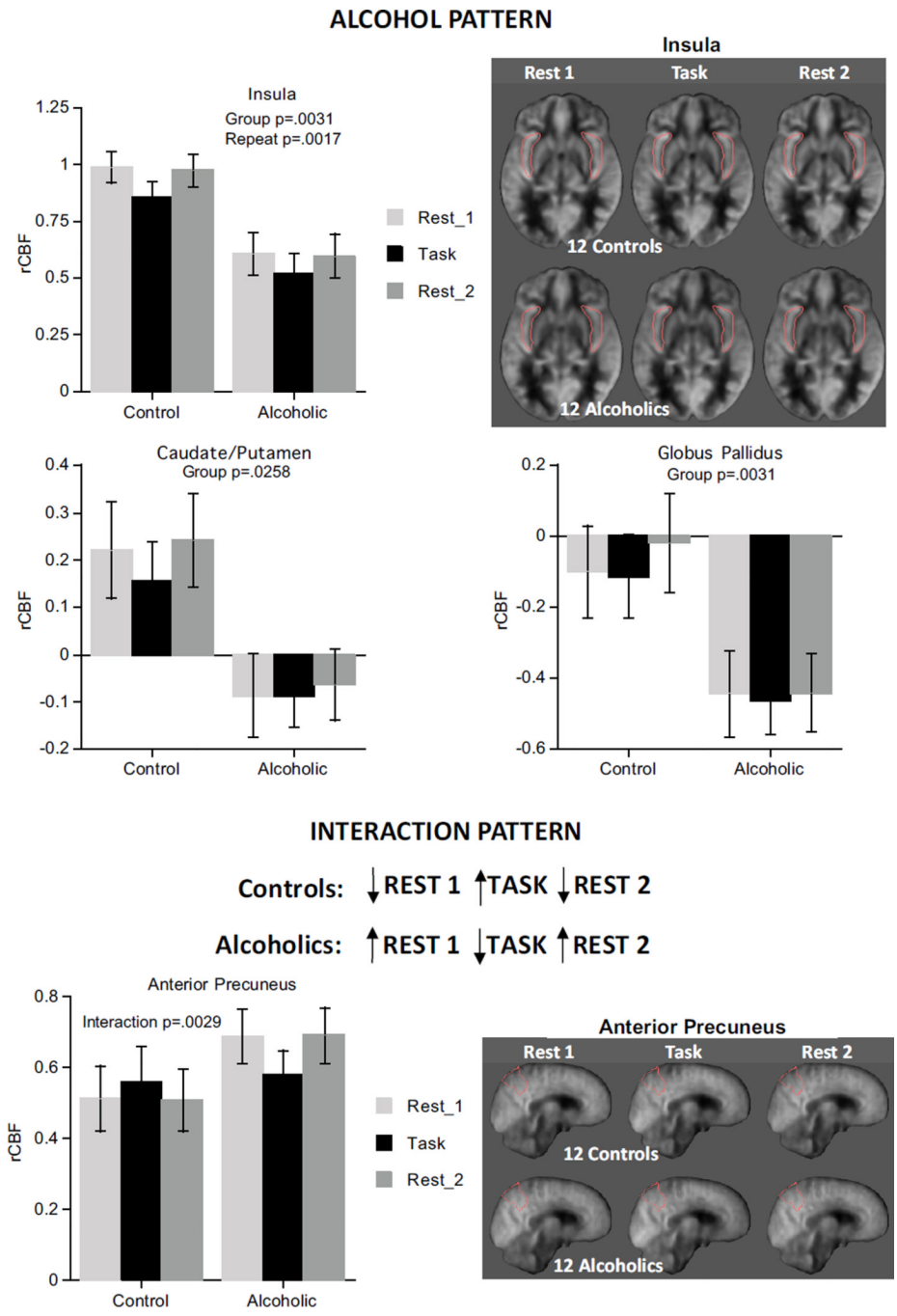

Figure 3.
Top: Alcoholic pattern evident from ANOVA. Bottom: Interaction pattern evident from ANOVA.

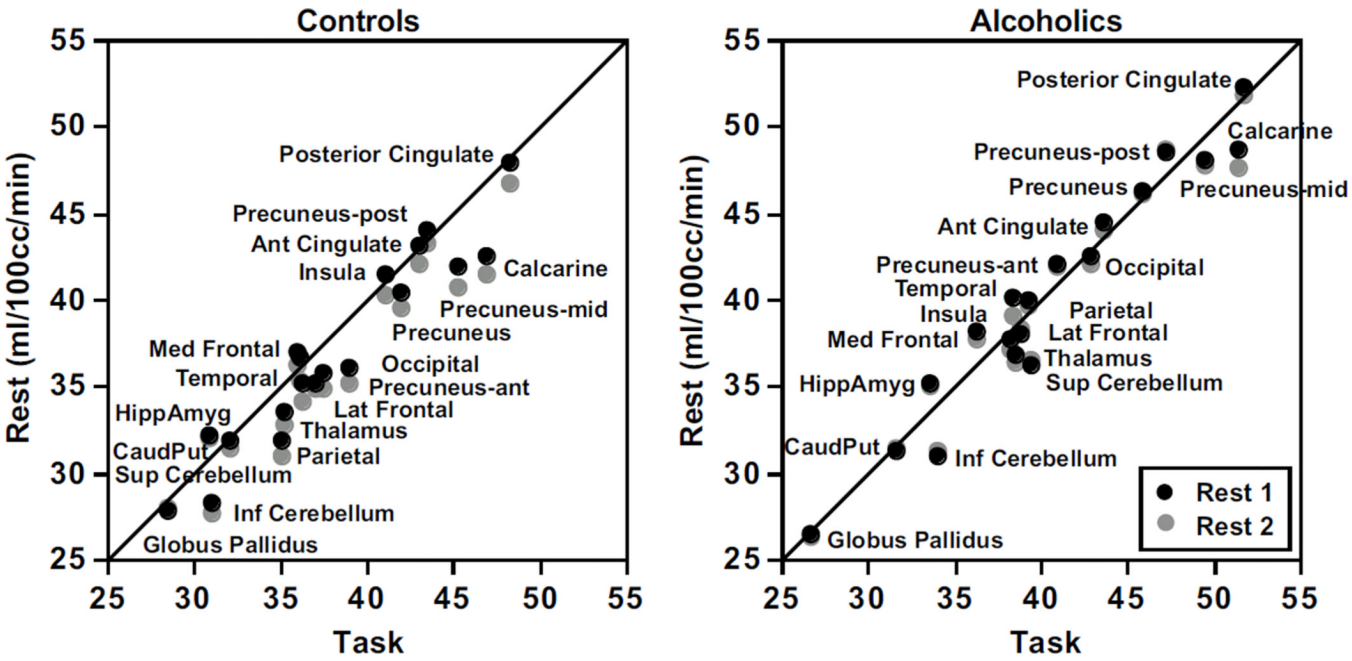

Figure 4.
Relations between rCBF at each rest condition and the task condition for the controls (left panel) and alcoholics (right panel).

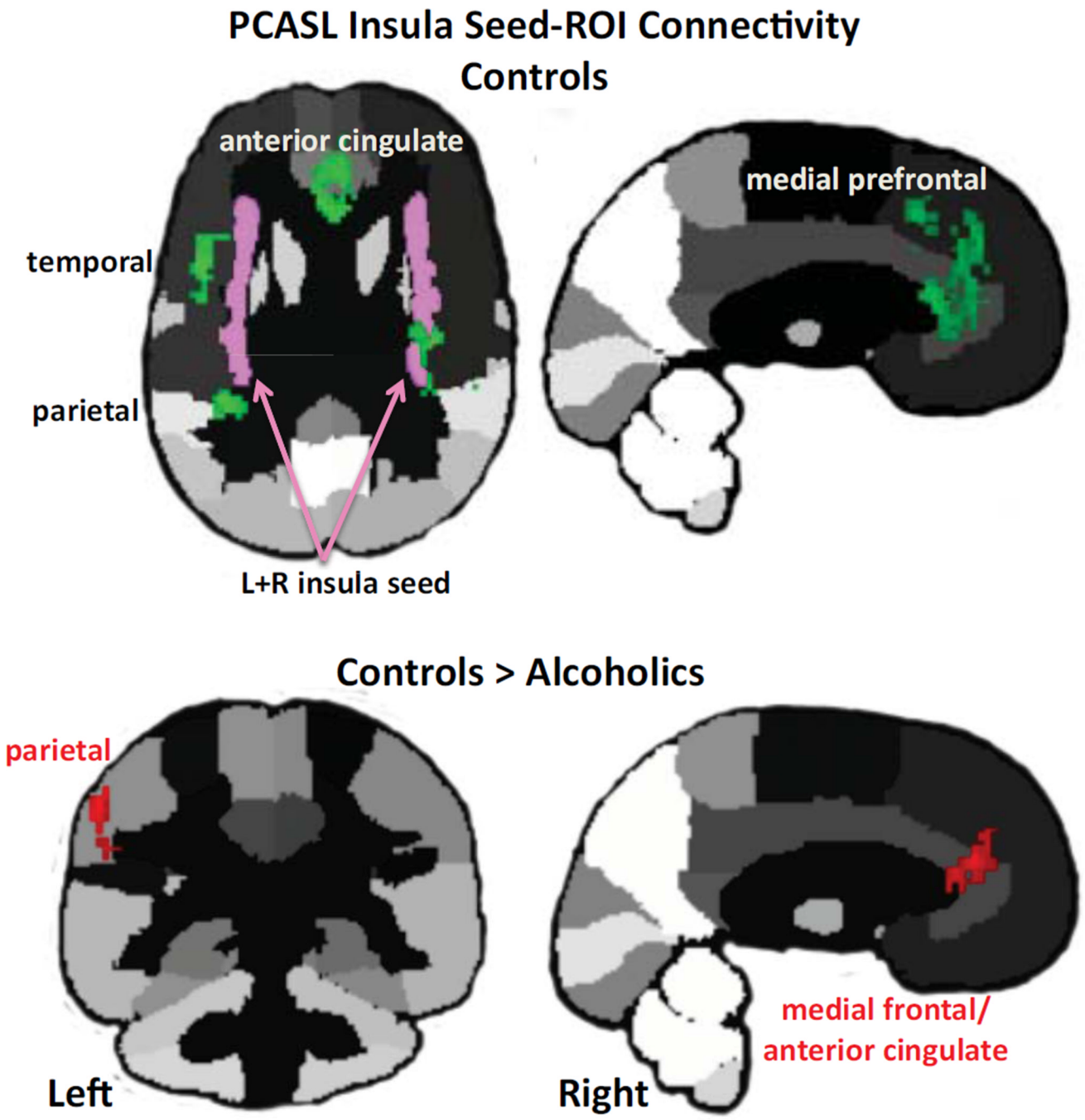

Figure 5.
Insula seed-to-ROI-connectivity results in controls (green) and between-groups comparison (red). Please refer to Table S3 in Supplement 1 for statistics.

Table 1

Group characteristics: mean (SD or range)

	Age (years)	Education (years)	Handedness	Lifetime Alcohol (kg)	Smoker	Smoking Onset Age (year)
Controls (12 men)	46.3 −5.2	16.9 −3.4	11R, 1L	34.1 −34.6	0	–
Alcoholics (12 men)	45.7 −4.4	12.9 −2.7	9R, 2L, 1A	1223.5 −790.9	8 current 1 past	23 (14 to 24)
t-test or c2 p-value	n.s.	0.005	n.s.	0.0005	0.01	

Alcoholics: sober for 31–539 days, except for one (sober for 1 day, no alcohol in blood).
Subjects refrained from smoking and drinking caffeinated beverages for at least 2 hours before PCASL acquisition.

Biol Psychiatry. Author manuscript; available in PMC 2014 October 01.